Stem Cell Reports
Report
ISSCR
OPEN ACCESS

Long-Term Safety, Immunologic Response, and Imaging Outcomes following Neural Stem Cell Transplantation for Pelizaeus-Merzbacher Disease

Nalin Gupta,[1,7,*] Roland G. Henry,[2,3,4] Sang-Mo Kang,[5] Jonathan Strober,[2,7] Daniel A. Lim,[1] Tamara Ryan,[6] Rachel Perry,[6] Jody Farrell,[6] Mary Ulman,[7] Raja Rajalingam,[8] Allyson Gage,[9] Stephen L. Huhn,[9] A. James Barkovich,[2,3,7] and David H. Rowitch[1,7,10]

[1]Department of Neurological Surgery, University of California San Francisco, 550 16th Street, 4th Floor, San Francisco, CA 94143-0137, USA
[2]Department of Neurology, University of California San Francisco, San Francisco, CA 94143, USA
[3]Department of Radiology and Biomedical Imaging, University of California San Francisco, San Francisco, CA 94143, USA
[4]Bioengineering Graduate Group, University of California San Francisco & Berkeley, San Francisco, CA 94143, USA
[5]Division of Transplantation, Department of Surgery, University of California San Francisco, San Francisco, CA 94143, USA
[6]Fetal Treatment Center, University of California San Francisco, San Francisco, CA 94143, USA
[7]Department of Pediatrics, University of California San Francisco, San Francisco, CA 94143, USA
[8]Immunogenetics and Transplantation Laboratory, Department of Surgery, University of California San Francisco, San Francisco, CA 94143, USA
[9]StemCells Inc., Newark, CA 94560, USA
[10]Department of Paediatrics, University of Cambridge, Cambridge CB2 1TN, UK
*Correspondence: nalin.gupta@ucsf.edu
https://doi.org/10.1016/j.stemcr.2019.07.002

SUMMARY

Four boys with Pelizaeus-Merzbacher disease, an X-linked leukodystrophy, underwent transplantation with human allogeneic central nervous system stem cells (HuCNS-SC). Subsequently, all subjects were followed for an additional 4 years in this separate follow-up study to evaluate safety, neurologic function, magnetic resonance imaging (MRI) data, and immunologic response. The neurosurgical procedure, immunosuppression, and HuCNS-SC transplantation were well tolerated and all four subjects were alive at the conclusion of the study period. At year 2, all subjects exhibited diffusion MRI changes at the implantation sites as well as in more distant brain regions. There were persistent, increased signal changes in the three patients who were studied up to year 5. Two of four subjects developed donor-specific HLA alloantibodies, demonstrating that neural stem cells can elicit an immune response when injected into the CNS, and suggesting the importance of monitoring immunologic parameters and identifying markers of engraftment in future studies.

INTRODUCTION

Pelizaeus-Merzbacher disease (PMD) is a rare, congenital X-linked recessive leukodystrophy caused by a mutation of the *proteolipid protein 1* (*PLP1*) gene (Gencic et al., 1989), resulting in reduced levels of myelination without an inflammatory component or substantial volume loss of brain tissue (Schiffmann and van der Knaap, 2009). PMD is one of a group of hypomyelinating disorders (Helman et al., 2015), with an incidence of 1:200,000–500,000. The severity of the disease is variable, but a subset of patients is affected by an early-onset severe form of PMD (also referred to as the connatal form) characterized by early nystagmus and profound neurodevelopmental deficits.

The primary biological deficiency in affected patients with PMD is the failure of oligodendrocytes to properly myelinate axons, resulting in axonal degeneration and neurological dysfunction. The genetic changes found in PMD include both gene duplications and point mutations of *PLP1* (Pouwels et al., 2014), resulting in abnormal myelin production (Schneider et al., 1992), or abnormal trafficking in the endoplasmic reticulum of oligodendrocytes. Because *PLP1* is only expressed in oligodendrocytes of the CNS, the pathobiology of PMD is cell type-restricted, and cell replacement has been proposed as a potential therapeutic approach (Duncan et al., 2008).

Animal models relevant to PMD show a spectrum of hypomyelination, seizures, and early postnatal lethality (Dhaunchak et al., 2011; Lin and Popko, 2009). Transplantation of human glial progenitor cells into the brain of hypomyelinated *Shiverer* (*Shi*) mice functionally engraft, leading to donor-derived myelination (Windrem et al., 2008). Human CNS stem cells (HuCNS-SCs), also referred to as neural stem cells, exhibit the properties of self-renewal and multipotency *in vitro*, and have been shown to produce oligodendrocytes that generate compact myelin, normalize nodal organization, and result in functional axonal conduction velocities in the *Shi* mouse model (Cummings et al., 2005; Uchida et al., 2012).

HuCNS-SCs are human fetal-derived multipotent neural stem cells (CD133, nestin, and Sox2 positive) that are expanded in culture as neurospheres, then cryopreserved into master and working cell banks, from which patient lots were obtained for transplantation (Uchida et al., 2000). The HuCNS-SCs intended for transplant in the phase I study originated from a cell bank-derived single donor. The surgical procedure for HuCNS-SC transplantation was previously described (Gupta et al., 2012). In brief, a total dose of 3.0×10^8 HuCNS-SCs per subject, divided

into four aliquots of 7.5×10^7 cells, was injected into the anterior and posterior centrum semiovale on both sides. The immunosuppression regimen consisted of oral tacrolimus with a target level of 5–10 ng/mL for the first 28 days following transplant and then a lower target level of 2–5 ng/mL until the end of 9 months post-transplant. Mycophenolate mofetil was also administered for the first 28 days post-transplant.

Magnetic resonance (MR) techniques can be used to assess brain development; diffusion tensor imaging (DTI) can quantify changes in the magnitude and direction of water motion that result from myelination, and is routinely used in the clinical characterization of demyelinating diseases in humans, such as multiple sclerosis (Pouwels et al., 2014). DTI has also been used to quantify the extent of myelination and remyelination in experimental models of hypomyelinating disorders.

The long-term impact and safety profile of HuCNS-SC transplantation and immunosuppression is an important question, particularly since late tumor formation has been reported following cell transplantation (Amariglio et al., 2009). In this study, 5 years post-transplant all patients were alive. Although there was no evidence of tumor development or other long-term adverse clinical effects of stem cell transplantation, two of four subjects developed donor-specific human leukocyte antigen (HLA) alloantibodies, demonstrating that neural stem cells can elicit an adaptive immune response. We describe anatomic changes over time that reveal a spectrum of morphological differences between subjects with severe *PLP1* mutations, and that the development of MR imaging (MRI) markers, although not specific, could occur in the presence of accumulated myelin or axon tract organization.

RESULTS

Study Subjects

When enrolled, the subjects were between 6 months and 5 years of age. The diagnosis of PMD was confirmed by the presence of mutations in *PLP1*, the absence of myelination by MRI, and clinical manifestations of early-severe PMD, the latter characterized by the onset of documented nystagmus by 3 months of age, severe developmental delay, and failure to attain normal gross motor milestones within 6 months of age. The specific mutations were different in all four subjects but affected the second transmembrane domain of the protein in subjects 1 and 3, and the fourth transmembrane domain in subjects 2 and 4 (subject 1, 221G>A, subject 2, 730T>G; subject 3, 223A>C; subject 4, 728C>T). Subjects 1 and 3 required tracheostomy and gastrostomy tube placement shortly after birth. Subjects 1 and 3 were 16 and 14 months of age, respectively, at the time of study entry and were noted to have minimal or no antigravity motor movement. Subjects 2 and 4 were 3 and 5 years of age, respectively, at the time of study entry and showed antigravity strength throughout, marked dysmetria, and minimal truncal support. Subject 4 also had the capability of very limited walker use with significant support. Subjects 2 and 4 were generally interactive with the ability to create some sounds or single words, as well as follow one-step commands, at study entry.

Clinical Outcomes

There was substantial variation in the clinical progression among the subjects (Table S1). Subject 1 showed no signs of neurological improvement, but his requirement for nightly continuous positive airway pressure (CPAP) was reduced over the course of 12 months following transplant. Subject 2 developed improved truncal support and the ability to take steps with assistance, and began speaking audible single words with the ability to follow two-step commands. Subject 3 developed antigravity strength in his upper extremities, started taking solid foods orally, and had reduced nightly CPAP requirements. Subject 4 developed improved truncal support and progressed from requiring significant support with use of the walker at baseline to walking with minimal assistance at the 12-month examination. Subject 4 also developed the ability to follow two-step commands and self-feed. No subjects developed seizure activity, and somatosensory evoked potential results did not change from baseline in any subject during the first year after transplant.

Ophthalmologic examination was performed at baseline prior to transplantation and during the long-term study. All subjects had visual impairment. Subject 1 showed severe optic nerve atrophy and an alternating exotropia that was stable. Subject 2 had mild-to-moderate optic atrophy, nystagmus, and myopia that was stable. Subject 3 had optic nerve atrophy and nystagmus, which appeared to be stable, but his visual behavior was noted to be worsened at the final 4-year time point. Subject 4 also had severe optic atrophy, nystagmus, and deterioration in visual behavior at the 4 year time point, with increased difficulty with fixation.

Immunologic Findings

To determine whether study subjects developed an immunologic response to HuCNS-SC transplantation, we analyzed serum samples collected before and each year after transplantation for HLA antibodies using the single-antigen bead Luminex assay. Two of the four subjects developed HLA antibodies including donor-specific antibodies (DSAs) during the follow-up period (Figure 1). Subject 1 developed 68 of 121 detectable core HLA alloantibodies (37 were directed to HLA class I allotypes; 31 were directed to HLA class II allotypes) at 1 year after transplant,

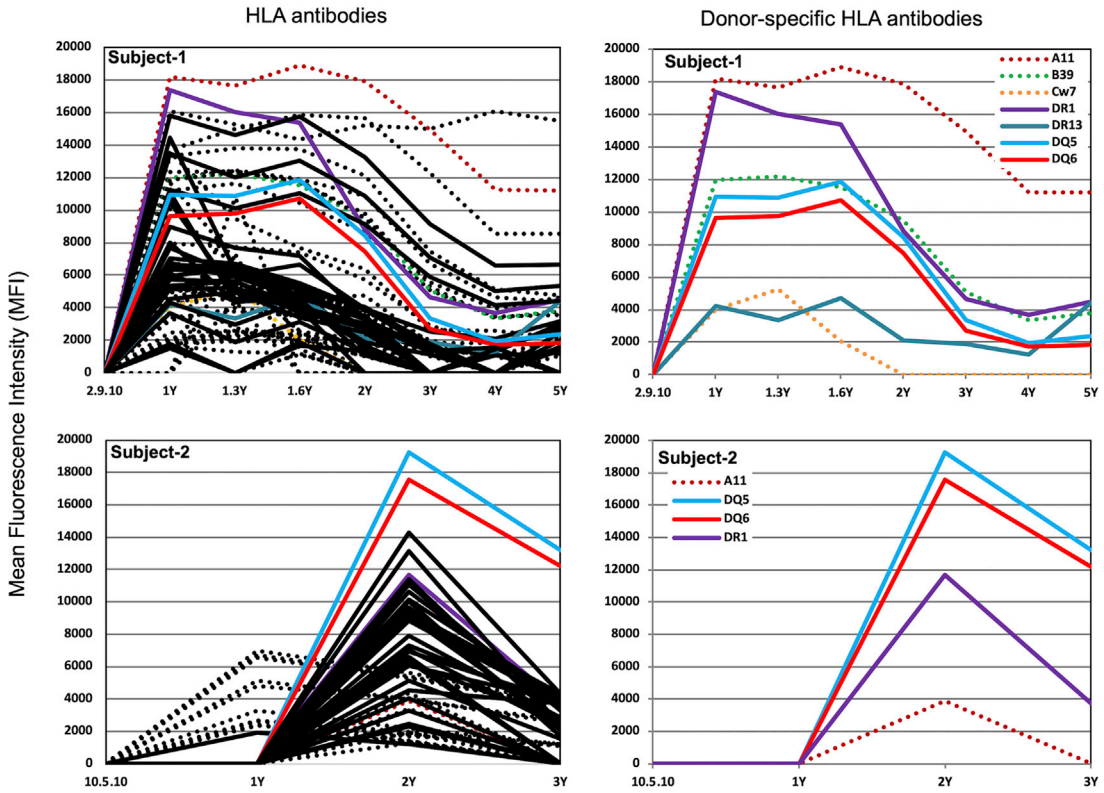

Figure 1. HLA Alloantibodies and HLA Donor-Specific Antibodies

Two of the four subjects receiving allogenic human neural stem cell transplants developed HLA autoantibodies and donor-specific antibodies (DSAs), while the two remaining subjects did not. The dotted lines indicate HLA class I alloantibodies, while the solid lines indicate HLA class II alloantibodies. The colored lines represent specific DSAs.

which include DSAs directed to all seven mismatched donors' HLA allotypes. Two years after transplant, the level of HLA alloantibodies dropped. Five years after transplant, 50% of the HLA antibodies were undetectable (only 17 class I antibodies and 15 class II antibodies were detected), but all except Cw7 DSAs persisted up to the 5-year time point. Notably, this patient had a subcutaneous collection of cerebrospinal fluid following the initial procedure, which might have potentiated systemic antigen exposure. Subject 2 had only 13 class I HLA alloantibodies at 1 year after transplant, and did not have a DSA at this time point (3 months after stopping immunosuppression). However, 2 years after transplantation, subject 2 generated five additional class I antibodies and 30 class I antibodies, of which four were DSAs. These data demonstrate that the stem cells elicited a classic alloantibody response after the cessation of immunosuppression, which is commonly seen after solid organ transplantation.

Imaging Findings

MRI studies, as part of the initial phase I component, were performed pre-transplant (baseline) and repeated at 3, 6, 9, 10, and 12 months post-transplant. Follow-up annual scans were acquired until 5 years post-transplant on three of the four subjects; however, subject 2 was only scanned for 2 years because the family could not return for evaluation. Post-contrast imaging was obtained yearly after transplantation during the study and no areas of increased enhancement were noted. MR spectroscopy was obtained but did not demonstrate any consistent changes over time.

Subjects 1 and 3 had progressive loss of diffuse white matter volume during the study, with associated ventriculomegaly such that the depths of some sulci were less than 2 mm from the ventricle in some locations. Cerebellar atrophy developed in the anterior lobe of the vermis in three subjects (mild in subjects 1 and 3; moderate to severe in subject 4).

Whole-brain fractional anisotropy (FA) increased (Figure 2A) and radial diffusivity (RD) decreased (Figure 2B) in all subjects. Whole-brain FA values for all patients followed an approximately quadratic growth while the RD followed a grossly quadratic decline (Figure 2C). Subjects 2 and 3 had similar age-matched FA and RD values, but subject 3 had higher levels of FA and subject 1 higher RD values

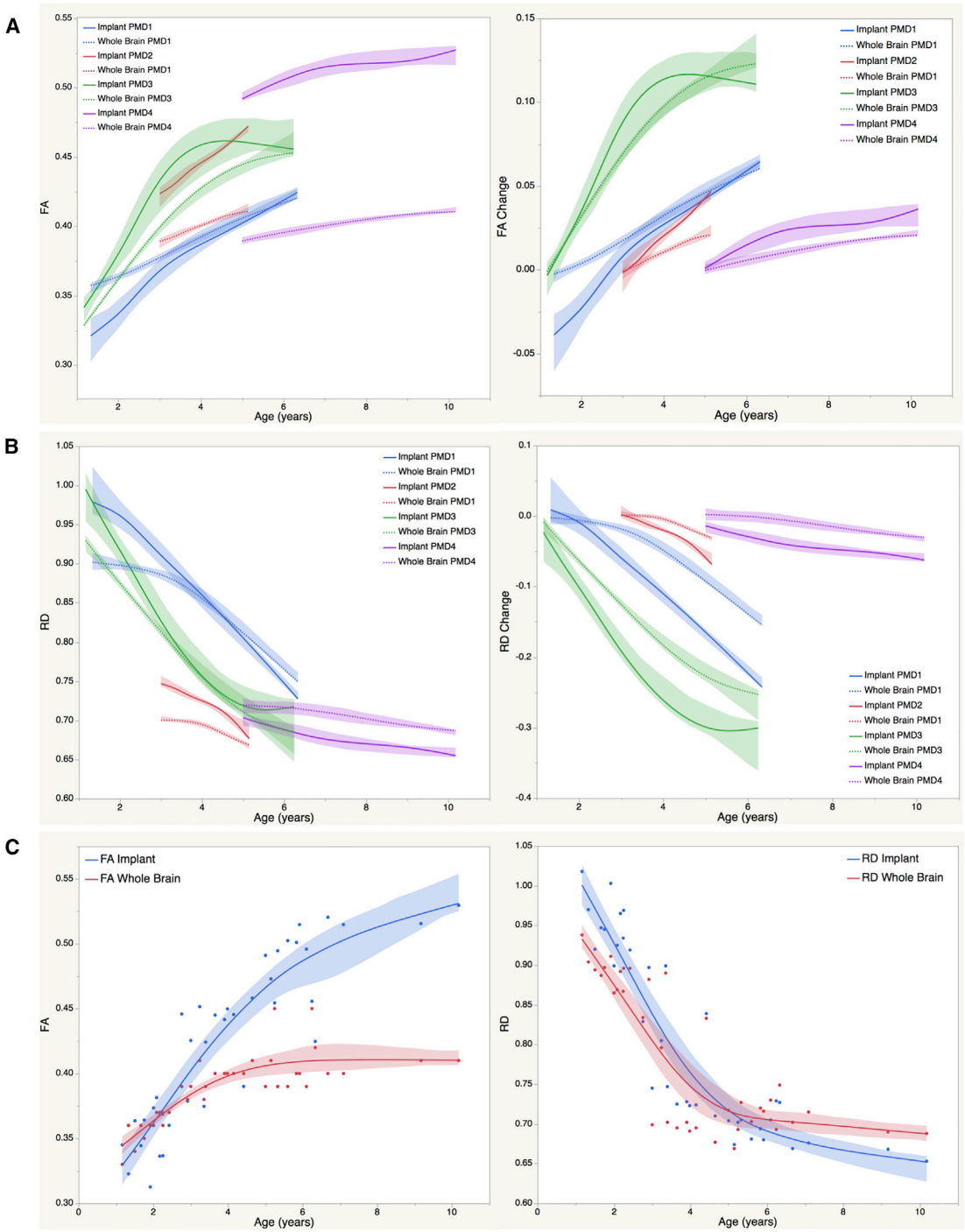

Figure 2. Fractional Anisotropy and Radial Diffusivity Shown as a Function of Subject Age

(A) Absolute fractional anisotropy (FA) values (left) and change in FA values (right) are shown for the implanted region (solid) and whole-brain (dashed). Error bars, represented as shaded colors, are 95% confidence intervals from fits using cubic splines. FA increased in all subjects over time for both implanted region and whole-brain. The whole-brain FA values were age consistent for three of the four subjects but higher for subject 3. Note that for subject 4, the implant region had significantly higher FA than the whole-brain at baseline. Changes in FA relative to baseline at 2 years post-transplant show that all four subjects had larger FA increases in the implant compared with whole-brain. At 5 years, this difference was diminished relative to whole-brain changes.

(legend continued on next page)

than the others. The implanted regions tended to have higher FA and higher RD values than the whole-brain, where the FA is increased due to higher axial diffusion coefficients (possibly related to axonal morphological or packing changes). Changes in FA from baseline suggest that the implanted regions at year 2 have larger FA increases compared with the whole-brain, but by year 5 the differences between implant and whole-brain FA values were not clearly significant. In contrast, changes in RD decreased faster in the implant than in whole-brain at both years 2 and 5. Larger reductions in RD and increases in FA were noted for the younger subjects. High-angular-resolution DTI data demonstrated increased FA throughout the areas of transplantation, with greatest change at the sites of the T1 and T2 shortening. This continued to evolve over time but was not seen in control regions several centimeters from the implantation sites.

DISCUSSION

Cell-replacement therapies have been proposed for treating of disorders of myelination, including diseases such as multiple sclerosis and cerebral palsy (Fancy et al., 2011). In contrast to hematopoietic stem cells, which lack any biological rationale for hypomyelinating disorders such as PMD (Goldman, 2016), neural stem cells have been shown to directly produce oligodendrocytes in animal models (Uchida et al., 2012). Here we report long-term findings of safety and other parameters 5 years following stem cell transplantation in a cohort of four subjects with PMD (Trepanier et al., 2010).

At baseline, the neurological and neuropsychological profiles of our subjects indicated severe and global CNS impairment. Although there were modest gains observed in three of the four subjects (and stability in the fourth subject) when viewed in the context of a progressive neurodegenerative disorder, there was evidence of disease progression in two of the subjects over the 4 years of the long-term study. However, these functional changes were not substantial enough to clearly indicate they resulted from the study intervention.

The immunologic findings reported in this study are the first, to our knowledge, to directly test for HLA alloantibody production after human-human neural cell engraftment. These results have important implications for future allogeneic neural stem cell transplantation trials. Our findings show that despite a low level of HLA expression, the neural stem cells can be subject to allorecognition by the recipient immune system. DSA can develop even in the presence of moderate immunosuppression, as seen in subject 1, but are not conclusive for donor cell rejection in the CNS. No MRI signature consistent with local inflammation was detected in any of the subjects. Notably, the development of DSA at least 3 months after the cessation of immunosuppression in subject 2 is quite suggestive of durable neural stem cell engraftment. Interpretation of the DSA response in our study is limited by the small number of subjects, but may support consideration of more potent and/or chronic immunosuppression in allogeneic neural stem cell therapies. Monitoring for DSA will be important in future studies in order to indicate potential rejection of the cells if there are no clear markers of engraftment, correlated with signs of clinical efficacy and refining immunosuppressive regimens and the feasibility of future allogeneic or even autologous transplant studies.

Qualitative T1- and T2-weighted morphologic images were taken in regions where the implantations took place in two of four subjects (Figure 3). However, these changes were patchy and subtle and could not be interpreted conclusively as evidence of myelination. There were increases in the T1 signal intensity (suggesting increased binding of water from increased cellularity and possible early myelin development) of the basal ganglia and thalami, but it varied in each individual. Subject 2 had the most profound changes, with nearly uniform T1 hyperintensity developing in the basal ganglia, thalami, and anterior and posterior limbs of the internal capsules (Figure 3), while subject 4 had changes nearly as profound in the deep gray nuclei but slightly less pronounced in the capsules. In contrast, subject 3 had high T1 signal develop in the caudates and putamina, but had patches of lower T1 signal in the globi pallidi while most of the lateral thalami were of low signal intensity. Fluid-attenuated inversion

(B) Radial diffusivity (RD) values (left) and change in RD values (right) as a function of age for implanted region (solid) and whole-brain (dashed). Error bars are 95% confidence intervals from fits using cubic splines. RD decreased in all subjects over time for both implanted region and whole-brain. The subjects had consistent age-specific values except for subject 1 whose RD values were higher throughout most of the study period, but approached the others at 5 years post-transplant. Changes in RD for whole-brain (dashed) and implant region (solid) relative to baseline at 2 years post-transplant for all four subjects had larger RD decreases in the implant compared with whole-brain, which persisted out to 5 years.

(C) Data from all subjects are plotted for FA (left) and RD (right) versus age, showing implanted (blue) and whole-brain (red) values. The fit is a cubic b-spline with lambda = 1.0, and the 95% confidence interval for the fit line is shaded. Overall FA values increase faster in the implanted region compared with the values obtained from the whole-brain. Similarly, there is a faster decrease in RD values in the implanted region compared with the whole-brain.

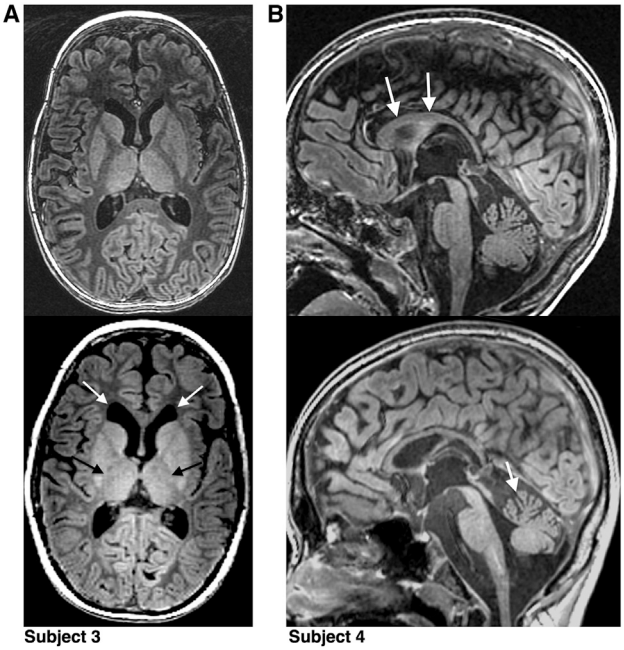

Figure 3. MRI over Study Interval for Subjects 3 and 4

(A) Axial T1-weighted MR image from subject 3 shows hypointensity, indicating a complete absence of myelin, in the white matter including the internal capsules. Follow-up axial T1-weighted image 5 years later (bottom image) shows high signal in the internal capsules, particularly of the posterior limbs (black arrows). Overall loss of white matter is seen in the frontal lobes with consequent enlargement of the frontal horns of the lateral ventricles (white arrows).

(B) Sagittal T1-weighted MR image from subject 4 shows that the anterior corpus callosum (white arrows) has nearly normal thickness. The posterior callosum is too thin and the anterior cerebellar vermis is atrophic. Follow-up sagittal T1-weighted image (bottom image) shows interval thinning of the anterior corpus callosum; the atrophy (small gyri and enlarged fissures) in the anterior cerebellar vermis (white arrow) has progressed.

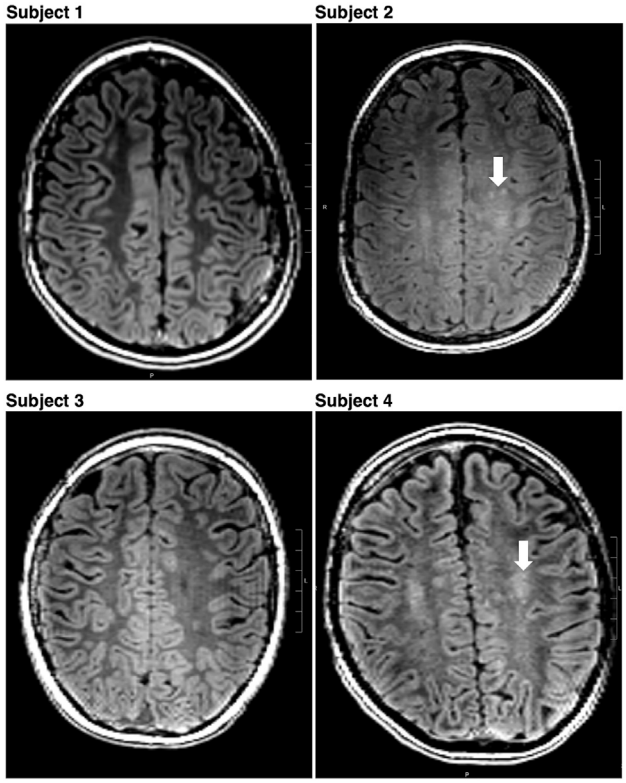

Figure 4. MR Images of the Regions of Implantation for All Four Subjects

Axial FLAIR images from subjects 1 to 4 (top left to bottom right), obtained 5 years following transplantation (except for subject 2, whose final study scan was done 3 years after transplantation). There are subtle, patchy areas of increased signal intensity noted in subjects 2 and 4 (arrows).

recovery (FLAIR) sequences demonstrated patchy areas of increased signal in the areas of transplantation in two subjects (Figure 4), but these changes were unspecific.

Animal models have revealed that myelination produces typical changes in quantitative DTI; specifically, increased FA and reduced RD (Uchida et al., 2012). Our results, when viewed individually and as a composite and compared with non-implanted regions, demonstrate a greater increase of FA in implant regions and a greater decrease in RD (Figure 2C; Tables S2 and S3). However, a clear limitation of this study is that other potential alternatives could also account for the observed DTI changes: inflammation, gliosis, abnormal proliferation, or increased numbers of axons. In addition, PMD has a variable phenotype, and the changes noted could also be occurring in the context of disease evolution and the subject's brain maturation. While DTI cannot identify specific biological inferences, it is possible that gliosis in implanted regions, together with myelination, may represent a potential (but not unique) interpretation of these results. In conclusion, the results of this long-term study demonstrate that the described stem cell transplantation intervention was safe and tolerated by subjects with PMD, but does not provide definitive evidence for transplant-related myelination over the natural history of maturation in these four subjects.

EXPERIMENTAL PROCEDURES

Study Approvals

The initial study of HuCNS-SC implantation was conducted between January 2010 and February 2012 as an open-label phase I trial in four subjects with the early-severe form of PMD (ClinicalTrials.gov NCT01005004). The US Food and Drug Administration (FDA)-authorized study protocol had oversight from the

Committee for Human Research (CHR) and Gamete, Embryo and Stem Cell Research Committees at University of California, San Francisco (UCSF). All four subjects were subsequently included in a prospective observational study that included clinical and radiologic endpoints, but did not have any therapeutic interventions. The long-term study was conducted under a separate protocol approved by the UCSF CHR. The families of all study subjects provided written informed consent.

Donor-Specific HLA Antibody Identification

HLA antibodies were measured using a Luminex-based LABScreen single-antigen bead (SAB) assay (One Lambda, Canoga Park, CA) according to the manufacturer's instructions. In brief, 5 μL of LABScreen HLA class I or II SAB beads were incubated with 20 μL of patient's serum in a 96-well format. Unbound excess serum was removed by washing the beads in the wells. One hundred microliters of phycoerythrin-conjugated goat antihuman immunoglobulin G antibodies were added to the wells for detection. The plates were incubated in the dark on a rotating platform for 30 min at room temperature, spun down at 2,800 rpm, and washed two times, followed by a Luminex instrument reading. Evaluations are carried out with the HLA fusion software. The results are expressed as adjusted median fluorescence intensity (MFI). Antibody specificity was determined based on known cross-reactivity patterns and MFI >1,000. Donor-specific HLA antibodies were identified by comparing the patient's HLA antibody specificity profile with the HLA types of the donor.

Cranial Imaging Techniques

All MRI/MR spectroscopy studies were performed on GE 3T MR scanners (General Electric Health Care, Milwaukee, WI, USA) with 8-channel phase array head coil and included volumetric T1 images (infrared spoiled gradient recall; repetition time [TR] = 11.58 ms, echo time [TE] = 4.8 ms, inversion time = 450 ms, partition size = 0.895 mm, in-plane resolution = 0.41 mm) and T2 images (volumetric fast-spin echo; TR = 4.0 s, TE = 104 ms, contiguous 1.5-mm sections, in-plane resolution = 0.94 mm). High-angular-resolution diffusion MRI data were acquired for DTI analyses (b = 2,000 s/mm^2, 55 directions, TR/TE = 15,000/74 ms, 2-mm isotropic voxels). Proton MR spectroscopy was performed within 4 × 2 × 2-cm voxels located in the bilateral centrum semiovale. Both short-echo (TR = 1,500 ms, TE = 26 ms) and long-echo (TR = 1,500 ms, TE = 288 ms) sequences were acquired.

SUPPLEMENTAL INFORMATION

Supplemental Information can be found online at https://doi.org/10.1016/j.stemcr.2019.07.002.

AUTHOR CONTRIBUTIONS

N.G., R.G.H., J.S., S.L.H., A.J.B., and D.H.R. were involved in the design and implementation of the clinical study. R.G.H., T.R., R.P., J.F., M.U., and A.G. were involved in study procedures and data acquisition. R.R. contributed to analysis of data. N.G., R.G.H., R.L.G., S.M.K., J.S., D.L., S.L.H., A.J.B., and D.H.R. analyzed the data and participated in writing the manuscript.

ACKNOWLEDGMENTS

R.G.H. receives research funding from Sanofi Genzyme, Roche/Genentech, Medday. Consultancy from Novartis, Medday, Roche, Sanofi-Genzyme, AbbVie, and Educational programs from Sanofi-Genzyme and TEVA. This clinical study was supported by StemCells, Inc.

Received: November 12, 2018
Revised: July 4, 2019
Accepted: July 5, 2019
Published: August 1, 2019

REFERENCES

Amariglio, N., Hirshberg, A., Scheithauer, B.W., Cohen, Y., Loewenthal, R., Trakhtenbrot, L., Paz, N., Koren-Michowitz, M., Waldman, D., Leider-Trejo, L., et al. (2009). Donor-derived brain tumor following neural stem cell transplantation in an ataxia telangiectasia patient. PLoS Med. *6*, e1000029.

Cummings, B.J., Uchida, N., Tamaki, S.J., Salazar, D.L., Hooshmand, M., Summers, R., Gage, F.H., and Anderson, A.J. (2005). Human neural stem cells differentiate and promote locomotor recovery in spinal cord-injured mice. Proc. Natl. Acad. Sci. U S A *102*, 14069–14074.

Dhaunchak, A.S., Colman, D.R., and Nave, K.A. (2011). Misalignment of PLP/DM20 transmembrane domains determines protein misfolding in Pelizaeus-Merzbacher disease. J. Neurosci. *31*, 14961–14971.

Duncan, I.D., Goldman, S., Macklin, W.B., Rao, M., Weiner, L.P., and Reingold, S.C. (2008). Stem cell therapy in multiple sclerosis: promise and controversy. Mult. Scler. *14*, 541–546.

Fancy, S.P., Chan, J.R., Baranzini, S.E., Franklin, R.J., and Rowitch, D.H. (2011). Myelin regeneration: a recapitulation of development? Annu. Rev. Neurosci. *34*, 21–43.

Gencic, S., Abuelo, D., Ambler, M., and Hudson, L.D. (1989). Pelizaeus-Merzbacher disease: an X-linked neurologic disorder of myelin metabolism with a novel mutation in the gene encoding proteolipid protein. Am. J. Hum. Genet. *45*, 435–442.

Goldman, S.A. (2016). Stem and progenitor cell-based therapy of the central nervous system: hopes, hype, and wishful thinking. Cell Stem Cell *18*, 174–188.

Gupta, N., Henry, R.G., Strober, J., Kang, S.M., Lim, D.A., Bucci, M., Caverzasi, E., Gaetano, L., Mandelli, M.L., Ryan, T., et al. (2012). Neural stem cell engraftment and myelination in the human brain. Sci. Transl. Med. *4*, 155ra137.

Helman, G., Van Haren, K., Bonkowsky, J.L., Bernard, G., Pizzino, A., Braverman, N., Suhr, D., Patterson, M.C., Ali Fatemi, S., Leonard, J., et al. (2015). Disease specific therapies in leukodystrophies and leukoencephalopathies. Mol. Genet. Metab. *114*, 527–536.

Lin, W., and Popko, B. (2009). Endoplasmic reticulum stress in disorders of myelinating cells. Nat. Neurosci. *12*, 379–385.

Pouwels, P.J., Vanderver, A., Bernard, G., Wolf, N.I., Dreha-Kulczewksi, S.F., Deoni, S.C., Bertini, E., Kohlschutter, A., Richardson, W., Ffrench-Constant, C., et al. (2014). Hypomyelinating

leukodystrophies: translational research progress and prospects. Ann. Neurol. *76*, 5–19.

Schiffmann, R., and van der Knaap, M.S. (2009). An MRI-based approach to the diagnosis of white matter disorders. Neurology *72*, 750–759.

Schneider, A., Montague, P., Griffiths, I., Fanarraga, M., Kennedy, P., Brophy, P., and Nave, K.A. (1992). Uncoupling of hypomyelination and glial cell death by a mutation in the proteolipid protein gene. Nature *358*, 758–761.

Trepanier, A.M., Bennett, L., and Garbern, J.Y. (2010). Pelizaeus-Merzbacher Disease: Natural History and Progression (American College of Medical Genetics).

Uchida, N., Buck, D.W., He, D., Reitsma, M.J., Masek, M., Phan, T.V., Tsukamoto, A.S., Gage, F.H., and Weissman, I.L. (2000). Direct isolation of human central nervous system stem cells. Proc. Natl. Acad. Sci. U S A *97*, 14720–14725.

Uchida, N., Chen, K., Dohse, M., Hansen, K.D., Dean, J., Buser, J.R., Riddle, A., Beardsley, D.J., Wan, Y., Gong, X., et al. (2012). Human neural stem cells induce functional myelination in mice with severe dysmyelination. Sci. Transl. Med. *4*, 155ra136.

Windrem, M.S., Schanz, S.J., Guo, M., Tian, G.F., Washco, V., Stanwood, N., Rasband, M., Roy, N.S., Nedergaard, M., Havton, L.A., et al. (2008). Neonatal chimerization with human glial progenitor cells can both remyelinate and rescue the otherwise lethally hypomyelinated shiverer mouse. Cell Stem Cell *2*, 553–565.